ELSEVIER

Journal of Non-Crystalline Solids 263&264 (2000) 263–270

JOURNAL OF NON-CRYSTALLINE SOLIDS

www.elsevier.com/locate/jnoncrysol

Synthesis and properties of niobium barium phosphate glasses

J.R. Martinelli *, F.F. Sene, L. Gomes

Brazilian Nuclear Energy Commission, Energy and Nuclear Research Institute, C.P. 11049 Pinheiros, CEP 05422-970, Sao Paulo, SP, Brazil

Abstract

Niobium barium phosphate glasses were prepared by melting different compositions of P_2O_5–Nb_2O_5–BaO–K_2O in an induction furnace. Three routes of preparation were adopted: (a) the material was melted at 1300°C, cast in a stainless steel mould and cooled to room temperature with a rod placed in contact with the upper surface of the liquid; (b) poured into the mould without the rod, (c) just removed from the furnace and cooled. Samples were prepared by varying the concentration of Nb_2O_5 from 0 to 40 mol%, BaO from 10 to 40 mol%, K_2O from 5 to 30 mol% and maintaining 30 mol% of P_2O_5. X-ray diffraction and thermal analyses were performed to determine if these materials were amorphous, the temperature of the crystallization peak (635–780°C) and the crystalline phase melting temperature (825–950°C). The glass transition temperature for the sample P_2O_5 30 mol%, Nb_2O_5 30 mol%, BaO 30 mol% and K_2O 10 mol% is 660 ± 5°C and the thermal expansion coefficient is $(11.68 \pm 0.5) \times 10^{-6}$ C^{-1}. The addition of BaO and consequently reduction of K_2O increase the temperature of the crystallization peak from 662°C to 838°C. Most of the studied compositions are amorphous only if the liquid is quenched. The sample of composition previously mentioned did vitrify when cooled in a crucible withdrawn from the furnace. Optical transparent glasses were produced and absorption bands in the range of 400–2500 nm were not detected. Absorption increased monotonically at wavelengths less than 380 nm.

1. Introduction

Phosphate glasses have been investigated since their use in processing of radioactive materials and the use of ionizing radiation when optical materials that could absorb γ- and X-rays were required [1]. At that time phosphate glasses were already known by their chemical durability related to their hydrolysis. Therefore their applications were restricted to smallest humidity environments.

The addition of iron in lead phosphate glasses increased chemical durability and the corrosion rate in aqueous environments could be sufficiently reduced to allow the use of this material in the immobilization and disposal of various types of radioactive nuclear waste [2]. Several works have reported advantages in processing this material, such as processing temperature and viscosity of the liquid [3,4]. However, some difficulties have also been reported if this material is proposed to be used in the nuclear waste disposal process, such as incompatibility with the existing processes developed for borosilicate glasses and the compositional limits of the phosphate based material to remain amorphous after cooling [5,6].

By replacing iron with indium or scandium, optical glasses with transparency in the visible range, refractive index, $1.75 \leqslant n \leqslant 1.83$ and dis-

* Corresponding author. Tel.: +55-11 816 9346; fax: +55-11 816 9370.

E-mail address: jroberto@net.ipen.br (J.R. Martinelli).

0022-3093/00/$ - see front matter
PII: S0022-3093(99)00638-9

persion smaller than that of silicate glasses could be obtained [7], even though PbO was still added as modifier. These materials had better chemical durability. The use of these materials as glass fibers and laser hosts was proposed [8]. A neodymium-doped athermal phosphate laser of exceptional optical quality and high gain with minimum beam divergence after repetitive use has been developed and is commercially available [9].

Niobium phosphate glasses have been previously investigated [10]. Several compositions have been prepared and properties measured [10]. These compositions contained PbO as a modifier. These glasses were stable at temperatures less than 800°C, which was attributed to units such as O–Nb–O and chemical durability attributed to Nb_2O_5 [10]. Niobium phosphate glasses have been used as glass planar optical waveguides fabricated by ion exchange [11].

In the present work PbO was replaced by BaO in phosphate glasses containing K_2O to avoid the volatility of lead oxide, reduce the environment impact due to lead processing and to investigate new compositions. Glasses were prepared by varying the composition to obtain chemically durable glasses, improved optical and thermal properties. X-ray diffraction patterns were recorded to determine their amorphous state. Differential thermal analysis (DTA), helium picnometry and optical absorption were measured to determine the onset and maximum crystallization temperatures, absolute density and absorption in the infrared range, respectively.

2. Experimental procedure

Precursor compounds such as $(NH_4)_2HPO_4$, Nb_2O_5, KOH and $BaCO_3$ were weighed and dry mixed with different compositions. Table 1 shows the batch composition. No measurement was performed to determine compositions after melting, since previously work performed on niobium phosphate glasses and lead iron phosphate glasses showed that there was no loss of K and P during the melting process [10,12].

In the present work each material composition is identified as PNBK followed by the corresponding concentration in mol% of P_2O_5, Nb_2O_5, BaO and K_2O, respectively.

Table 1
Batch composition (mol%)

Composition/compound	P_2O_5	Nb_2O_5	BaO	K_2O
1	30	30	10	30
2	30	20	20	30
3	30	30	30	10
4	30	40	10	20
5	30	10	40	20
6	30	05	45	20
7	30	30	35	05
8	30	25	15	30
9	30	–	40	30

Mixtures were melted in an induction furnace in an alumina crucible inside a graphite crucible to heat the alumina crucible from room temperature to the melting temperature. A rotating system was used to homogenize the melt. A flow of argon reduced graphite oxidation. A batch was initially heated to 450°C at 20°C/min and soaked for 10 min to decompose $(NH_4)_2HPO_4$ to P_2O_5. Consequently, ammonia and water were released. The batch was then heated to 1300°C at 20°C/min. The melt was homogenized by spinning the crucible and soaked for 30 min. Finally the liquid was cast in a stainless steel mould and a stainless steel rod was placed in contact with the upper surface of the liquid to cool it at an estimated cooling rate of 35°C/s. The material was then pushed from the mould and immediately annealed at 480°C in air for 2 h to relieve internal stresses. This temperature was chosen based on previous experimental results and, it is in the range of temperature where viscosity is 10^{13} Poise for this system. This procedure we named the fast-cooling route. Some liquids were poured into the stainless steel mould without the rod in contact with the upper surface and then annealed. In this case the estimated cooling rate was 18°C/s. Some spherical drops were made and called slow-cooled samples. Some materials were prepared by just removing the alumina crucible from the furnace. In this case, the cooling rate was 10°C/min.

Powder samples were prepared for X-ray diffraction analyses, by grinding in a mortar with a pestle. A diffractometer (Bruker–AXS model D8-

Advance) was used. Samples were scanned from 10° to 120° at 2°C/min. CuK_α radiation was used.

Samples were prepared for DTA by grinding in a mortar with a pestle and sieving in a 48 mesh sieve. Particles smaller than 300 μm were used for DTA (Netzsch simultaneous thermal analysis model STA 490 c/7/E). A flow of air was maintained during the analysis and samples were heated from room temperature to 1000°C at 10°C/min.

Samples were also prepared for optical absorption. Glass pieces were cut, ground with SiC particles 1000 mesh over a commercial glass surface, washed in distilled water by using ultrasound, polished with diamond paste from 15 μm down to 6 μm in a polishing machine (Panambra model PanTec). Samples were then washed again in distilled water with ultrasound and finally dried in air. No reaction between water and glass was visually observed.

Optical absorption measurements were performed by using a spectrophotometer (Cary/Olis model 17D) in the region of 200–2500 nm.

The linear refractive index (n_o) was determined by a refractometer (Carl Zeiss Abbe). The wavelength used for this purpose was 589 nm, which corresponds to the strongest intensity of the sodium emission spectrum. Samples were cut in laminae with parallel surfaces. A liquid with a refractive index larger than the measured one was used as a second medium.

A dilatometer (Netzsch model 402) was used to determine the transition temperature (T_g) and the thermal expansion coefficient. The temperature ranged from room temperature to 700°C at 5°C/min. Air was used as the atmosphere during the measurement.

Densities were determined by using a helium pycnometer (Multivolume Micromeritics model 1305).

3. Results

3.1. Glass preparation

For the materials prepared by the fast-cooling route, the surface contact is greater and the cooling is more uniform. Solidified drops are avoided. Samples obtained by slow-cooling route are opaque and whitish for most compositions, except compositions PNBK 30–30–30–10 and PNBK 30–30–35–05. By using the fast-cooling route, samples transparent in the visible range, yellowish and bubble free were obtained for compositions PNBK 30–30–10–30, PNBK 30–20–20–30, PNBK 30–30–30–10 and PNBK 30–40–10–20. In the other compositions, crystallization was observed. Cooling rate and composition were the main factors related to the glass formation. In the slow-cooling route, molecular mobilization and rearrangement (nucleation and growth of crystalline phases) are possible. For fast-cooled materials, glass formation was possible. However some specific compositions form glasses even if cooled inside the crucible, as observed for PNBK 30–30–30–10 and PNBK 30–30–35–05, shown latter in a compositional diagram.

3.2. Differential thermal analysis

Fig. 1 shows the DTA for a sample with composition PNBK 30–20–20–30. Two exothermic peaks are resolved. The crystallization peak temperatures and melting temperature (endothermic peak) are 635°C ± 5°C, 780°C ± 5°C and 824°C ± 5°C, respectively. Similar results were obtained for the whitish opaque samples. X-ray diffraction analysis shows that these samples are partially

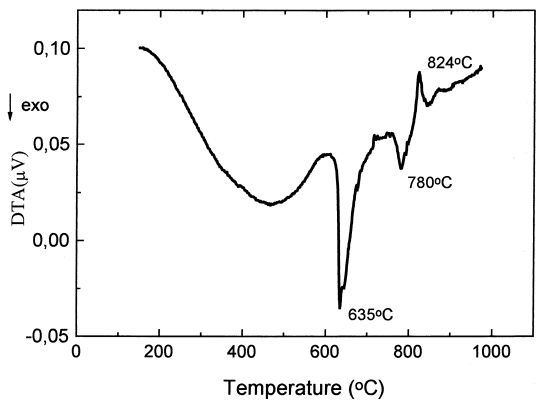

Fig. 1. DTA for samples with composition PNBK 30–20–20–30 fast-cooled.

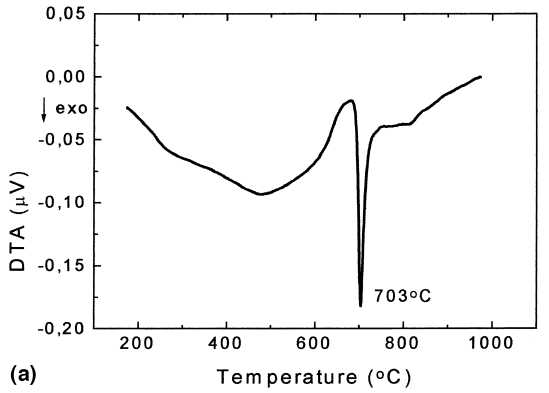

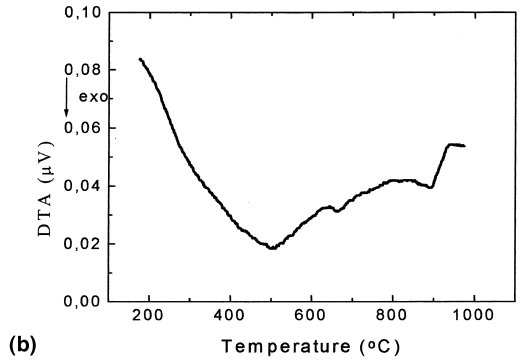

Fig. 2. DTA for samples with composition PNBK 30–30–10–30 cooled by different routes: (a) fast-cooling, (b) slow-cooling.

crystallized (see below). The glass transition temperatures were not determined by DTA

Fig. 2 shows the DTA for fast-cooled samples with composition PNBK 30–30–10–30 (Fig. 2(a)) and for samples cooled inside an alumina crucible used to melt the glass components (Fig. 2(b), slow-cooling). Two samples were used for each measurement. The fast-cooled glass had an exothermic peak at 703°C ± 5°C determined by the DTA which we assume to be due to crystallization because this material shows X-ray diffraction peaks related to crystalline phases above this temperature.

Fig. 3 shows the DTA for a fast-cooled sample (laminate shape). The DTA of samples slow-cooled (spherical drop shape), is similar.

Table 2 shows the temperature of crystallization peaks for different compositions in the DTA curves.

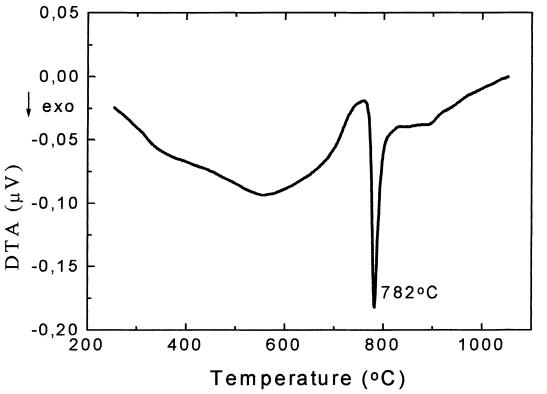

Fig. 3. DTA for samples with composition PNBK 30–30–30–10 prepared by fast-cooling.

Table 2
Temperature (T_c) of crystallization peaks in the DTA curve

Composition PNBK	T_c (°C)
30–25–10–35	662 ± 5
30–30–10–30	703 ± 5
30–30–30–10	778 ± 5
30–30–35–05	838 ± 5

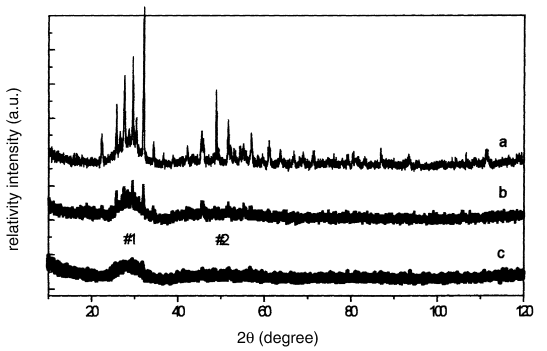

Fig. 4. X-ray diffraction pattern for samples PNBK 30–20–20–30: (a) cooled inside the crucible, (b) slow-cooled in a mold, (c) fast-cooled.

3.3. X-ray diffraction

Fig. 4 shows the X-ray diffraction pattern of samples PNBK 30–20–20–30 prepared by: (a) melting and cooling inside alumina crucibles, (b) slow-cooled in a stainless steel mold and (c) fast-cooled, respectively.

Table 3
Density for materials with composition PNBK 30–20–20–30

Processing route	Density (g/cm^3)
Slow-cooled in crucible	3.680 ± 0.001
Fast-cooled in steel	3.502 ± 0.001
Slow-cooled in steel	3.561 ± 0.001

For samples with composition PBNK 30–30–30–10 and PNBK 30–30–35–05 slow-cooled inside the alumina crucible, the X-ray diffraction pattern is similar to that in Fig. 4(c). No X-ray diffraction peaks related to crystalline phases were detected.

3.4. Density

Table 3 gives the densities, determined by He picnometry for samples with composition PNBK 30–20–20–30 prepared by different routes: (1) the melt was slow-cooled inside an alumina crucible; (2) optical transparent sample prepared by fast-cooling; and (3) opaque sample prepared by slow-cooling. Since the objective of these measurements was primarily to determine the effects of preparation routes on the crystallization, no additional measurements were done for other compositions.

3.5. Compositional diagram

From the above data and visual observation, we construct a preliminary compositional diagram showing compositions that lead to glass structures or crystalline phases after fast-cooling. Fig. 5 shows a diagram of the different compositions studied in the present work.

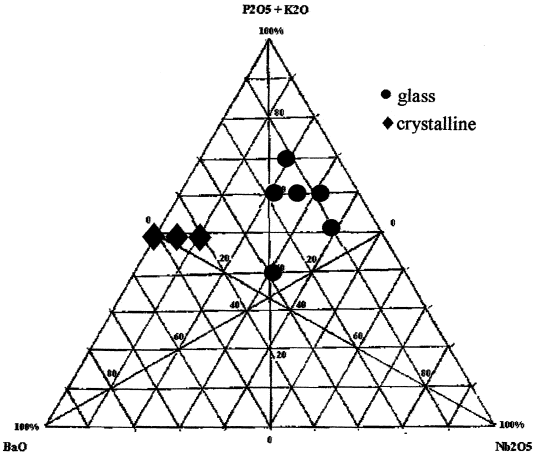

Fig. 5. Diagram representing compositions studied in the present work: (●) amorphous, (◆) crystalline.

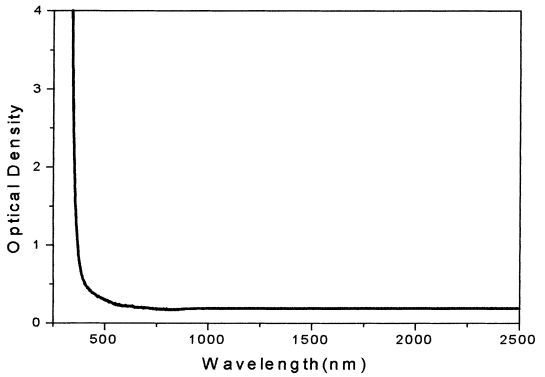

Fig. 6. Optical absorption curve.

3.6. Optical absorption

Fig. 6 shows optical absorption as a function of wavelength for a sample PNBK 30–30–30–10. This sample was 1.3 mm thick. No measurements were made on samples of other compositions, since PNBK 30–30–30–10 was the most promising material for optical applications.

3.7. Linear refraction index and dilatometric analysis

The linear refractive index for samples with composition PNBK 30–30–30–10 is 1.79 ± 0.05 at 589 nm. The thermal expansion coefficient measured for one sample with this same composition is $(11.685 \pm 0.005) \times 10^{-6}$ C^{-1} in the temperature range of 350–510°C and the T_g is 660 ± 5°C. The error was estimated according to the precision of the dilatometer. This measurement was done only for this composition.

3.8. Emission spectroscopy

Table 4 shows the concentration of the major metallic elements determined by emission spec-

Table 4
Concentration of metallic elements in the raw materials and in the glass

Element	$(NH_4)_2HPO_4$ (± 5 ppm)	Nb_2O_5 (± 5 ppm)	$BaCO_3$ (± 5 ppm)	KOH (± 5 ppm)	Glass PNBK 30–30–30–10 (± 5 ppm)
Co	45	45	45	45	45
Ni	45	45	45	45	45
Cr	45	45	45	45	45
Cu	15	15	15	15	15
Ti	–	–	–	–	–
V	30	30	30	30	15
Mn	100	15	15	15	80
Fe	75	75	75	75	75
Al	60	60	60	60	3000

troscopy for each compound used to synthesize a glass with composition PNBK 30–30–30–10. Impurities in glass sample measured by emission spectroscopy are also shown in this table.

4. Discussion

4.1. Differential thermal analysis

Samples prepared by slow-cooling did not have an exothermic peak in the DTA data that could be associated with a crystallization process; hence this absence is an indication that the material was crystallized, before the DTA measurement, during cooling from the liquid state. No endothermic peak was observed to indicate melting of any crystalline phase in the investigated range of temperature. Therefore, melting of crystalline phases are at temperatures higher than 950°C (maximum temperature of these analyses). Fig. 1 shows two exothermic peaks related to crystalline phases nucleation. Fig. 2(a) shows that, for more homogeneous glasses, only one exothermic peak related to crystalline nucleation and growth is observed.

Compositions PNBK 30–30–30–10 and PNBK 30–30–35–05 are glassy even when the liquid is cooled inside the crucible. X-ray diffraction patterns for these compositions do not have peaks that could be related to crystalline phases. The glass transition temperature was determined to be 660 ± 5°C by dilatometric analysis of these compositions.

In spite of the fact that from Table 2 we note the variation of the crystallization peak temperatures as a function of barium, niobium and potassium concentrations, we can only infer that by increasing the amount of barium and decreasing the amount of potassium, the temperature of crystallization peak increases. Barium ionic radius is larger than the other elements in these glasses and can inhibit the relaxation that leads to crystallization. Therefore BaO is a modifier that increases the viscosity and reduces the nucleation and growth rates for crystalline phases. When potassium is added to phosphate glasses, the network is disrupted, the ion mobility increases and crystallization is made easier.

For samples PNBK 30–25–10–35 and PNBK 30–30–10–30, the amount of barium was kept constant and potassium varied from 35 to 30. We observed that the temperature of the crystallization peak decreases when potassium concentration increases. However, it is difficult to separate the effects of each component in a complex system because we have to change the concentration of other elements simultaneously to keep the total molar concentration. For instance, to vary the concentration of potassium we chose to vary the concentration of niobium because we were interested to study the effects of barium. The niobium effects on the peak crystallization temperature is already known. Niobium is a glass former in phosphate glasses and the temperature of crystallization peak increases as the niobium concentration increases [10].

4.2. X-ray diffraction

The samples could be classified on the basis of their X-ray diffraction as: (A) predominantly crystalline, (B) partially amorphous and (C) fully amorphous.

Samples prepared by slow-cooling in a steel mold had diffraction peaks and halos in the diffraction pattern related to crystalline and amorphous phases (Fig. 4(b)). We classify these materials as B-type. Samples prepared by fast-cooling in a steel mold had diffraction patterns of amorphous phases and therefore short range order structures produce the halos #1 and #2 in the X-ray diffraction pattern and we classify them as C-type (Fig. 4(c)). Halo #1 is due to $Ba_4O(PO_4)_2$ and $NbPO_5$ since the X-ray diffraction peaks for crystalline phases related to these compounds are located in the same Bragg's angle range where this halo is observed (JCPDS files). Halo #2 is due to the $Ba_4O(PO_4)_2$ structure for the same reason.

Peaks corresponding to crystalline phases from PNBK 30–30–10–30 can be identified (Fig. 4(a)). This material can be classified as A-type.

No peaks related to crystalline phases are detected in the X-ray diffractograms of samples of PNBK 30–30–30–10 prepared by fast- or slowcooling. This composition has the smallest tendency for crystallization. This composition also forms glasses irrespective of the preparation route and different shapes such as laminates, spherical drops and rods can be obtained.

4.3. Density

The sample with composition PNBK 30–20–20–30 cooled inside the alumina crucible is predominantly crystalline and has the largest density. The same composition prepared by fast-cooling has the smallest density. The opaque material (PNBK 30–20–20–30) prepared by slow-cooling in a steel mold is partially crystalline and has an intermediate density.

4.4. Optical absorption

No bands in the visible and infrared range were observed (400–2.500 nm) in a sample of PNBK 30–30–30–10. An absorption was observed at wavelengths less than 380 nm. The absorption coefficient was 40.17 cm^{-1} at 350 nm.

4.5. Emission spectroscopy

As it can be seen from Table 4, the composition which forms a glass irrespective of the preparation route has larger concentration of aluminum, indicating that the liquid was contaminated by the alumina crucible during melting. This sample also contained 80 ppm of manganese from the $(NH_4)_2PO_4$, which may be the source of light yellowish color [13].

Physical properties such as density, refractive index, coefficient of thermal expansion and T_g were determined only for the C-type samples that did not crystallize and could be obtained even at the smallest cooling rates in our experiment.

5. Conclusions

Considering the range of transparency, the glass PNBK 30–30–30–10 can be used as a host material for (3+) rare-earth ions, leading to possible new laser materials, having in mind the infrared optical transitions.

Acknowledgements

The authors thank The Brazilian National Research Council CNPq for a scholarship granted to F.F. Sene and Mr Solon Tagusagawa (Companhia Brasileira de Metalurgia e Mineração), for kindly providing niobium oxide. DTA analysis were performed in an equipment granted by FAPESP Project 95-5172/4. X-ray diffraction were performed in an equipment granted by FAPESP Project 96-9604/9.

References

[1] J.J. Rothermel, K.-H. Sun, A. Silverman, J. Am. Ceram. Soc. 32 (5) (1949) 153.
[2] B.C. Sales, L.A. Boatner, Science 226 (1986) 45.

[3] B.C. Sales, L.A. Boatner, in: W. Lutze, R.C. Ewing (Eds.), Radioactive Waste Forms for the Future, Elsevier, Amsterdam, 1988, p. 193.
[4] B.C. Sales, M.M. Abraham, J.B. Bates, L.A. Boatner, J. Non-Cryst. Solids 71 (1985) 103.
[5] L.A. Chick, L.R. Bunnell, D.M. Strachan, H.E. Kissinger, F.N. Hodges, Advances in Ceramics (special issue), Nuclear Waste Management II 20 (1986) 149.
[6] C.M. Jantzen, Advances in Ceramics (special issue), Nuclear Waste Management II 20 (1986) 157.
[7] B.C. Sales, L.A. Boatner, J. Am. Ceram. Soc. 70 (9) (1987) 615.
[8] W.S. Key, J.C. Miller, ORNL Rev. 27 (3) (1994) 4.
[9] S.A. Payne, C.D. Marshall, A. Bayramian, G.D. Wike, J.S. Hayden, Appl. Phys. B 61 (1995) 257.
[10] N. Aranha, PhD thesis, Campinas State University, Chemical Institute, Brazil, 1994.
[11] N.V. Nikonorov, E.V. Kolobkova, M.B. Zakhvatova, Soviet J. Glass Phys. Chem. 19 (1) (1993) 66.
[12] S.T. Reis, PhD thesis, University of Sao Paulo, Brazil, 1999.
[13] J.M.F. Navarro, Consejo Superior de Investigaciones Científicas, Fundación Centro Nacional del Vidrio, Madrid, Spain, 1991.